Terahertz surface plasmon polaritons on a helically grooved wire

A. I. Fernández-Domínguez,[1,a)] C. R. Williams,[2] F. J. García-Vidal,[1] L. Martín-Moreno,[3] S. R. Andrews,[2] and S. A. Maier[4]
[1]*Departamento de Física Teórica de la Materia Condensada, Universidad Autónoma de Madrid, E-28049 Madrid, Spain*
[2]*Department of Physics, University of Bath, Bath BA2 7AY, United Kingdom*
[3]*Instituto de Ciencia de Materiales de Aragón and Departamento de Física de la Materia Condensada, CSIC-Universidad de Zaragoza, E-50009 Zaragoza, Spain*
[4]*Experimental Solid State Group, Physics Department, Imperial College, London SW7 2AZ, United Kingdom*

(Received 23 July 2008; accepted 4 September 2008; published online 10 October 2008)

The propagation of tightly confined terahertz surface plasmon polaritons on a helically grooved metal wire has been studied both experimentally and theoretically. The periodic structure of such *metawires* allows the formation of surface electromagnetic modes with different azimuthal symmetry at wavelengths longer than the pitch. There is good agreement between the experimentally determined band edge frequencies of these modes and numerical calculations for the structure investigated. © *2008 American Institute of Physics*. [DOI: 10.1063/1.2988897]

There has been recent interest in surface electromagnetic (EM) modes, known as surface plasmon polaritons (SPPs), for possible applications in guiding and sensing at terahertz frequencies.[1–3] For smooth metal surfaces in air, SPPs at these frequencies have attractively low dispersion, but the large spatial extent in air restricts the applications. Pendry *et al.*[4] outlined how the dispersion of surface EM modes can be engineered by surface texturing. They showed that even perfectly conducting *metamaterial* surfaces can sustain modes resembling SPPs, with an effective plasma frequency determined completely by the geometry. Surface structuring thus facilitates an extension of visible plasmonic concepts for subwavelength localization of EM energy[5] to frequencies significantly lower than the intrinsic plasma frequency of the conductor. In the technologically emergent terahertz regime, this creates opportunities for planar waveguides with high out-of-plane confinement and added functionality such as focusing or defect guiding.[6,7] For cylindrical geometries, there are some previous works from the 1950s[8] on low-frequency propagation on metallic wire structures. Very recently, we have demonstrated that strong confinement and focusing of the geometrically induced SPPs can be achieved by tuning the depth of the grooves in a cylindrical wire.[9] Here, we report an experimental demonstration of this SPP guiding on a helically grooved wire at terahertz frequencies, and present a theoretical analysis of the dispersion and azimuthal symmetry of the modes.

In our experimental setup, a 150 mm long helically grooved metawire was formed by tightly wrapping a steel wire (radius of 200 μm) around a 200 μm radius core. The assembly was then nickel plated. For comparison, we also studied a bare copper wire of the same outer radius (600 μm) and length. The wires were studied using time domain terahertz spectroscopy in which pulses of radially polarized broadband (~2 THz) radiation were generated by femtosecond optical excitation of an annular geometry GaAs photoconducting source.[2] The terahertz beam was collimated to a diameter of the order 6 mm using a silicon substrate lens and end-fire coupled to the wires whose ends were placed a few millimeters away from the tip of the lens. Radiation propagating off the opposite end of the wires was similarly coupled to a 50 μm long arsenic implanted dipole receiver. The wires were bent along the arc of a circle with radius of 26 cm to discriminate against unguided free space radiation.

Figure 1(a) shows time domain traces of the receiver current for the wires with smooth and helically grooved surfaces. It is apparent that a single-cycle-like pulse, the Sommerfeld wave,[10] propagates on the smooth wire and that

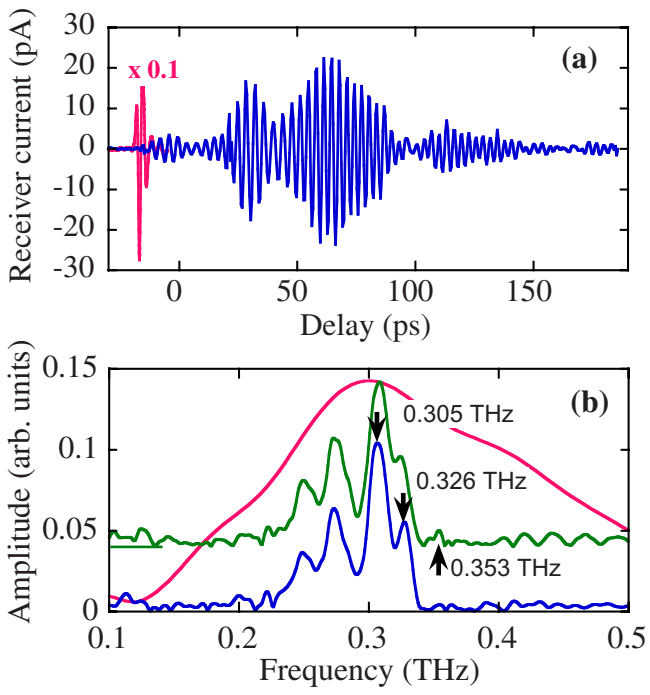

FIG. 1. (Color online) (a) Receiver current as a function of time delay for the smooth wire (red curve) and the helical groove structure (blue curve). (b) Amplitude spectra of the time domain data in (a) together with the spectrum of another nominally identical helical sample (green curve, displaced for clarity). The arrows indicate the three azimuthal modes of the helical groove structure. The spectrum of the Sommerfeld wave (red curve) on the smooth wire extends to ~1 THz.

a)Electronic mail: anisaac.fernandez@uam.es.

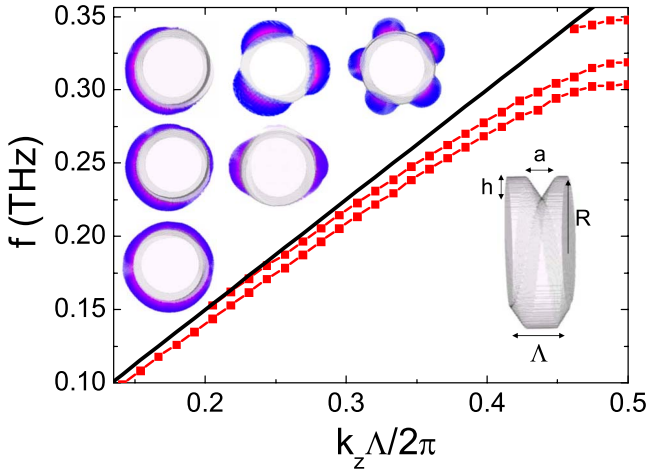

FIG. 2. (Color online) Dispersion relation of the surface EM modes supported by a PEC wire of radius $R=600\ \mu$m inscribed with a triangular cross-section helical groove of pitch $\Lambda=400\ \mu$m. The groove has width $a=200\ \mu$m and depth $h=150\ \mu$m. The upper row of insets displays electric field magnitude maps evaluated at the three band edges, $f_{BE}=0.305$ (left), 0.320 (center), and 0.349 THz (right). The next lower row corresponds to the first mode at 0.280 THz (left) and the second mode at 0.180 THz (right). The map in the lowest row is for the first mode at 0.180 THz.

propagation on the helical wire exhibits significant dispersion together with beating due to the presence of modes with different frequencies. Figure 1(b) shows the amplitude spectra of the traces in Fig. 1(a) together with the spectrum of a second, nominally identical sample of the helical structure, which exemplifies the reproducibility of the data to small variations in optical alignment. The vertical scale is the same for all three spectra. To a first approximation, the amplitude spectrum is proportional to the frequency dependent electric field of the guided modes at the end of the wire convolved, with the receiver response and the transfer function involved with radiation of the guided modes into free space and propagation to the receiver in the far field. The band edges (f_{BE}) of the three lowest frequency bound azimuthal modes are identified, with the aid of numerical calculations described below, as the peaks at 0.305 ± 0.002, 0.326 ± 0.002, and 0.353 ± 0.003 THz. The relative intensity of the peaks depends on the orientation of the receiver antenna as a result of the different azimuthal mode symmetries. The detected polarization has been chosen to clearly reveal the guided mode frequencies. The structure below 0.3 THz is associated with the propagation of radiation at smaller wave vectors and is discussed further below.

In Fig. 2, the bands associated with the surface EM modes obtained using the finite-difference-time-domain (FDTD) method are displayed. In these calculations, we assume that the metal behaves as a perfect electrical conductor (PEC), which is a good approximation at terahertz frequencies. In accordance with the experimental parameters, the helix pitch is $\Lambda=400\ \mu$m and the wire radius is $R=600\ \mu$m. The EM fields are evaluated inside a unit cell along the z-direction (parallel to the wire axis). The FDTD square mesh dimension is set to $5\ \mu$m. Due to design limitations, the modeled groove has a triangular profile of width a and depth h (see Fig. 2). We find that $a=200\ \mu$m and $h=150\ \mu$m give a good match to the experimental results for the f_{BE}. The main panel of Fig. 2 shows the bands for this set of geometrical parameters. Surface EM modes at the band edge are defined by the condition $k_z=\pi/\Lambda$, where k_z is the wave vector component along the z-direction. The three theoretical f_{BE} obtained from FDTD calculations, 0.305, 0.320, and 0.349 THz, are in excellent agreement with the highest frequency peaks found in the experimental amplitude spectra.

The insets of Fig. 2 show snapshots of the electric field magnitude $|E|$ of the surface EM modes supported by the metawire at various frequencies. Note that, as expected, the lack of azimuthal symmetry of the metallic structure leads to nonsymmetrical $|E|$ distributions. The upper row shows the electric field magnitude at the three f_{BE}, increasing in frequency from left to right. The fields are confined within less than a wavelength of the surface. The field maps shown in the lower two rows are evaluated at smaller k_z. The two left most ones correspond to the first surface mode at 0.280 and 0.180 THz, and that on the right of the second row to the second surface mode at 0.180 THz. We observe that at f_{BE}, the surface EM modes exhibit an odd number of azimuthal nodes (1, 3, and 5), whereas with decreasing k_z, the number of nodes is gradually reduced by one and becomes even. Thus, the surface EM modes propagating along the helical structure at low k_z resemble the case of a wire patterned with periodic arrays of annular grooves, where the number of nodes is even.[9]

We now analyze why the surface EM modes supported by the metawire exhibit such a k_z dependent azimuthal symmetry. Any component of the EM fields bound to a helical structure[11] can be expanded in terms of diffracted waves as $F_m(r,\theta,z)=e^{ik_z z}e^{im\theta}\Sigma_n A_{nm-n}(r)e^{in\left(\frac{2\pi}{\Lambda}z-\theta\right)}$, where the modal amplitude $A_{nm-n}(r)$ contains the radial dependence of the n^{th}-diffracted wave. $F_m(r,\theta,z)$ is an eigenfunction of the helical translation operator $S_{\phi\frac{\Lambda}{2\pi}\phi}$,[12] satisfying $S_{\phi\frac{\Lambda}{2\pi}\phi}F_m(r,\theta,z)=F_m\left(r,\theta+\phi,z+\frac{\Lambda}{2\pi}\phi\right)=e^{i\left(m+k_z\frac{\Lambda}{2\pi}\right)\phi}F_m(r,\theta,z)$, where index m controls the symmetry properties of the EM fields. We now introduce the helical coordinate $\xi=z-\frac{\Lambda\theta}{2\pi}$,[13] which is parallel to the cylindrical coordinate z, but measured from the surface $z=\frac{\Lambda\theta}{2\pi}$. EM fields can be expressed in terms of ξ as $F_m(r,\theta,\xi)=f(r,\xi)e^{i\left(m+k_z\frac{\Lambda}{2\pi}\right)\theta}$. It is now clear that this eigenfunction, evaluated along the helical surfaces $\xi=$constant, evolves in time as $\cos\left[\left(m+k_z\frac{\Lambda}{2\pi}\right)\theta-2\pi ft\right]$, where f and t are the mode frequency and time, respectively. Thus, snapshots of the EM fields with $k_z=\pi/\Lambda$ show $2m+1$ nodes along one helix pitch, whereas for $k_z=0$, they show only $2m$ nodes. We can label the surface EM modes in Fig. 2 with the indices $m=0$, $m=1$, and $m=2$.

We also carried out numerical simulations on an extended finite wire using a finite integration technique (FIT). As in the experiments, the helical structure is formed by wrapping a PEC wire of radius $200\ \mu$m around a straight cylindrical core of the same radius (see schematic picture in Fig. 3). The 9.6 cm long structure is illuminated in the near field with a radially polarized plane wave propagating parallel to the wire axis. Probes monitoring the longitudinal component of electric field (E_z) are located along the structure, close to the wire surface ($615\ \mu$m away from the wire axis), at four different azimuthal positions ($\theta=0$, $\pi/2$, π, and $3\pi/2$). Figure 3 shows the E_z field amplitude versus frequency recorded by the probes, which are located 1.5 cm away from the illuminated wire end. The simulation time

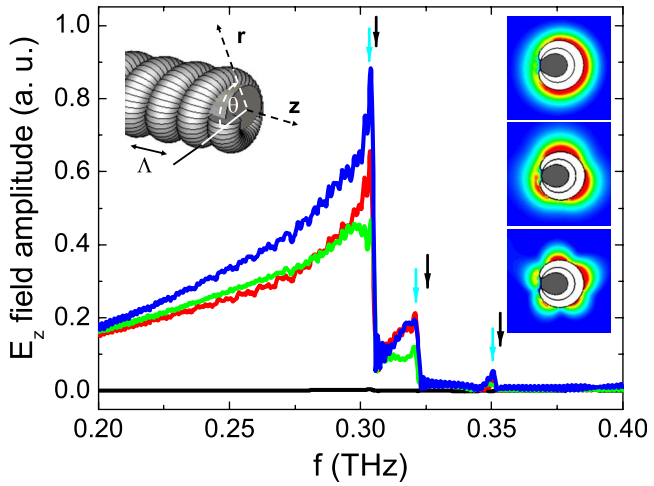

FIG. 3. (Color online) FIT simulations of the propagation of surface EM modes on a 9.6 cm long wire. The metawire is modeled as a PEC wire of radius 200 μm tightly wound on a straight PEC wire of the same dimensions. The helix pitch is $\Lambda=400$ μm. Main panel shows the spectra of E_z at four points close to the wire surface ($r=615$ μm, $\theta=0$, $\pi/2$, π, and $3\pi/2$) located 1.5 cm away from the illuminated end. Right insets show $|E_z|$ in a cross section at the three f_{BE} obtained from FDTD calculations (from top to bottom: 0.305, 0.320, and 0.349 THz). These frequencies are shown in the main panel by cyan arrows and the corresponding frequencies in the experimental spectra are indicated by black arrows.

(700 ps) is chosen so that reflection of the EM fields at the nonilluminated wire end is avoided. The spectrum resembles the experimental one except for the structure in the tails below 0.3 THz. The black vertical arrows indicate the position of the three experimental peaks, which are in excellent agreement with the maxima in the electric field amplitude close to the wire surface in our FIT simulations and in close correspondence with the band edge frequencies obtained from FDTD simulations (vertical cyan arrows). In order to confirm that the three maxima in the FIT spectra correspond to the excitation of guided modes on the structure, we also mapped the electric field amplitude in the plane containing the four field probes described above. The three insets on the right of Fig. 3 show the electric field patterns at the frequencies indicated by vertical cyan arrows in the main panel. The field patterns are consistent with the FDTD results, which demonstrate that the FIT spectral maxima are associated with the resonant excitation of the $m=0$, $m=1$, and $m=2$ surface EM modes.

The relative amplitudes of the spectral peaks reflect the efficiency with which the radially polarized incident mode is scattered into the guided modes and is similar to that observed experimentally. The modulation in amplitude below 0.3 THz observed experimentally in Fig. 1 does not appear in the long tail to lower frequency in the simulation shown in Fig. 3. We have taken care to exclude spectral artifacts associated with reflections or finite delay range in the experiment. We therefore tentatively assign this structure to either unintentional variations in the pitch of the metawire or, more likely, to the frequency dependence of the coupling of the guided modes to free space radiation, which is not explicitly modeled. Resolution of this problem is subject to ongoing investigations on structures with different geometrical parameters and will be reported in a future publication.

In conclusion, we have experimentally observed the excitation of terahertz frequency surface EM modes on a helically grooved wire and numerically modeled the propagation. We have been able to identify three modes with different azimuthal symmetry and shown how these evolve with wave vector component parallel to the direction of propagation. We expect that such grooved metawires will find applications as terahertz surface waveguides, sensors, or focusing devices.

This work was sponsored by the Royal Society, the Air Force Office of Scientific Research (Grant Nos. FA9550-07-1-0441 and FA8655-07-1-3045), and the Spanish MCyT under Grant No. MAT2005-06608-C02 and consolider NanoLight.es.

[1] K. Wang and D. M. Mittleman, Nature (London) **432**, 376 (2004).
[2] T.-I. Jeon, J. Zhang, and D. Grischkowsky, Appl. Phys. Lett. **86**, 161904 (2005).
[3] T.-I. Jeon and D. Grischkowsky, Appl. Phys. Lett. **88**, 061113 (2006).
[4] J. B. Pendry, L. Martín-Moreno, and F. J. García-Vidal, Science **305**, 847 (2004); F. J. García-Vidal, L. Martín-Moreno, and J. B. Pendry, J. Opt. A, Pure Appl. Opt. **7**, S97 (2005).
[5] W. L. Barnes, A. Dereux, and T. W. Ebbesen, Nature (London) **424**, 824 (2003); S. A. Maier, *Plasmonics: Fundamentals and Applications* (Springer, New York, 2007).
[6] S. A. Maier and S. R. Andrews, Appl. Phys. Lett. **88**, 251120 (2006).
[7] C. R. Williams, S. R. Andrews, S. A. Maier, A. I. Fernández-Domínguez, L. Martín-Moreno, and F. J. García-Vidal, Nat. Photonics **2**, 175 (2008).
[8] G. Goubau, J. Appl. Phys. **21**, 1119 (1950); W. Rotman, Proc. IRE **39**, 952 (1951); S. Sensiper, *ibid.* **43**, 149 (1955); G. Piefke, IRE Trans. Antennas Propag. **7**, 183 (1959).
[9] S. A. Maier, S. R. Andrews, L. Martín-Moreno, and F. J. García-Vidal, Phys. Rev. Lett. **97**, 176805 (2006).
[10] A. Sommerfeld, Ann. Phys. Chem. **303**, 233 (1899).
[11] P. J. Crepeau, Proc. IEEE **52**, 33 (1964).
[12] J. B. Knorr and P. R. McIsaac, IEEE Trans. Microwave Theory Tech. **19**, 854 (1971).
[13] R. A. Waldron, Q. J. Mech. Appl. Math. **11**, 438 (1958).